

ANALYSIS OF SOLAR INSOLATION AND SOLAR ENERGY PRODUCTION AT AN OKLAHOMA MESONET SITE

Zuleydian Roche-Rivera^{1,2}, Keith A. Brewster³, and Christopher A. Fiebrich⁴

¹National Weather Center Research Experiences for Undergraduates Program
Norman, Oklahoma

²University of Puerto Rico, Mayagüez
Mayagüez, Puerto Rico

³Center for Analysis and Prediction of Storms
Norman, Oklahoma

⁴Oklahoma Mesonet
Norman, Oklahoma

ABSTRACT

Renewable energy sources, including solar energy, present opportunities for sustained development and electrical generation with minor impacts on Earth. Solar energy systems are becoming more affordable and, despite Oklahoma's abundant sunny days each year, the solar energy field remains untapped. From April 2017 to April 2018, a field experiment was carried out at the Oklahoma Mesonet site at the National Weather Center to analyze the solar insolation and solar energy production. A solar panel was instrumented with its own pyranometer to measure the global downwelling solar radiation at a tilt angle of 47 degrees, along with solar panel temperature, current, and voltage. This experimental data was compared with the standard data set of the Mesonet site, where a seasonal variation was observed in the relationship between the horizontal solar radiation and the solar radiation at the tilted surface. A cubic equation defined the relationship between the observed power and the solar radiation at the solar panel. Using the relationship to estimate power, coupled with the observed power and the panel's temperature, we found no temperature dependency for the energy production efficiency in the solar panel.

1. INTRODUCTION

We live in a world that is striving to become more sustainable and develop cleaner sources of energy. It is believed that wind and solar radiation are two of the most abundant renewable energy sources, and they present opportunities for electrical generation with minor impacts on Earth (Li et al. 2011).

There are several studies that analyze the availability and variability of renewable energy production with the combination of solar photovoltaic (PV) power and wind power in a hybrid system (e. g., Brewster et al. 2016; Li et al.

2011; and Reichling et al. 2008). Brewster et al. (2016) assessed renewable energy potential across Oklahoma and concluded that wind power is less able than potential new solar energy facilities to meet energy production needs at the time of peak demand in that state. As of 2017, Oklahoma had 7,495 megawatts of installed wind power capacity (American Wind Energy Association 2017). On the other hand, Oklahoma has many sunny days each year, with daily accumulation of solar radiation ranging from 0.79 MJ/m² to 30.34 MJ/m² during 2017 and 2018 at Norman, OK. However, the solar energy production potential in the state remains largely untapped.

¹ *Corresponding author address:* Zuleydian Roche-Rivera, University of Puerto Rico at Mayagüez, HC 03 BOX 8041, Barranquitas, PR 00794, zuleydian.roche@upr.edu.

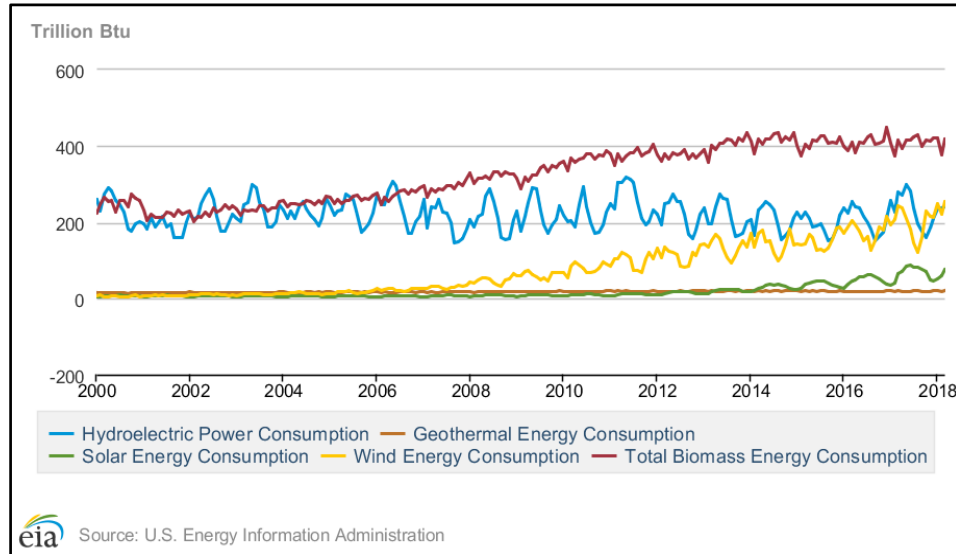


Figure 1: Renewable Energy Production and Consumption by Source over the years from the U. S. Energy Information Administration.

Over time, the cost of solar energy systems has dropped significantly (U. S. Department of Energy 2018). Even though the use of solar energy has become more affordable, the U. S. Energy Information Administration indicates the increase in solar energy consumption has not grown as quickly as other sources of energy (Fig. 1).

The Oklahoma Mesonet is a statewide network of automated environmental monitoring stations that provide regular weather data that are transmitted every five minutes to the Oklahoma Climatological Survey. The data quality are immediately verified and then made available to Mesonet users (Van der Veer Martens et al. 2017). Commissioned in 1994, the Oklahoma Mesonet has 25 years of data, including solar radiation, but it is not a simple process to go from the Mesonet observations to estimates of potential solar energy production.

Not all of the Mesonet’s sites have the instruments to record a data set for the analysis of solar energy production across Oklahoma. The purpose of this project is to couple the standard Mesonet observations with those from a field experiment to produce solar energy production estimates. We analyze the potential for solar energy production in central Oklahoma during peak demand times on critical days. We also compare the availability of solar energy during the different seasons of the year to see

how much solar radiation is received and, most importantly, how much power can be generated.

In this study, we are interested in the potential for solar energy production in a real-world environment. We focused on three key research questions: (1) How can we relate the Mesonet’s standard solar radiation data to the solar radiation incident to the tilted panel, (2) How does the observed solar radiation relate to the power generated from the solar panel, and (3) Since the efficiency of a solar panel can be affected by the temperature of the individual solar cells, what is the temperature dependence of the solar panel’s efficiency under different conditions.

2. DATA AND METHODS

For this project, data from a unique field experiment was analyzed. For one year (April 2017 – April 2018), a solar panel was instrumented with its own pyranometer, panel temperature sensor and a special device to record voltage and current measurements at the National Weather Center’s Mesonet site in Norman, Oklahoma.

The solar panel evaluated was a 13-year old BP SX 30-Watt Photovoltaic Module with a nominal power of 30 Watt, a Nominal Operating Cell Temperature (NOCT) of 47 °C, and a warranty of 90% power output over 12 years. It was instrumented with two Li-Cor LI-200SA pyranometer sensors that were used to measure

total global downwelling solar radiation averaged over five minutes intervals. One pyranometer was pointed vertically, as is the standard in the Oklahoma Mesonet, while the other was mounted at the same angle as the face of the solar panel (i.e., 47 degrees).

The optimum tilt angle of a solar panel is typically calculated by adding 15 degrees to the latitude during winter and subtracting 15 degrees from the latitude during summer (Duffie and Beckman, 1980). The Oklahoma Mesonet has the need to maximize the solar radiation during the winter months when the overall availability of solar energy is lower, due to sun angle and a cloudier climatology in the state. Because of our location's latitude of 35.236 degrees N, both the solar panel and the pyranometer were tilted at 47 degrees and faced south (Fig. 2).

From the Mesonet's standard data feed, we examined the global downwelling solar radiation (W/m^2) and the air temperature ($^{\circ}C$). From the experimental dataset, we utilized the solar radiation (W/m^2), the solar panel temperature ($^{\circ}C$), the current (A), and the voltage (V) observations. The dataset was nearly complete with only 3% loss due to a short-term battery failure and downtime during logger upgrades.

Each pyranometer was calibrated in the Oklahoma Mesonet lab and an optimal coefficient was determined (McPherson et al. 2007). Before using and analyzing the data obtained from both pyranometers, the calibration coefficients must be applied to the data in real-time during processing:

$$\text{Calibrated SRAD} = \frac{SRAD * 80}{\text{Calibration coef}} , \quad (1)$$

where $SRAD$ is the observed value for solar radiation in each pyranometer in W/m^2 . The calibration coefficient for the standard pyranometer is 62.4, and the one for the tilted pyranometer is 56.1.

It is possible to calculate the elevation angle of the sun based on the latitude of the site and day of the year:

$$\delta = 23.45^{\circ} \sin \left[\frac{360}{365} (284 + d) \right], \quad (2)$$

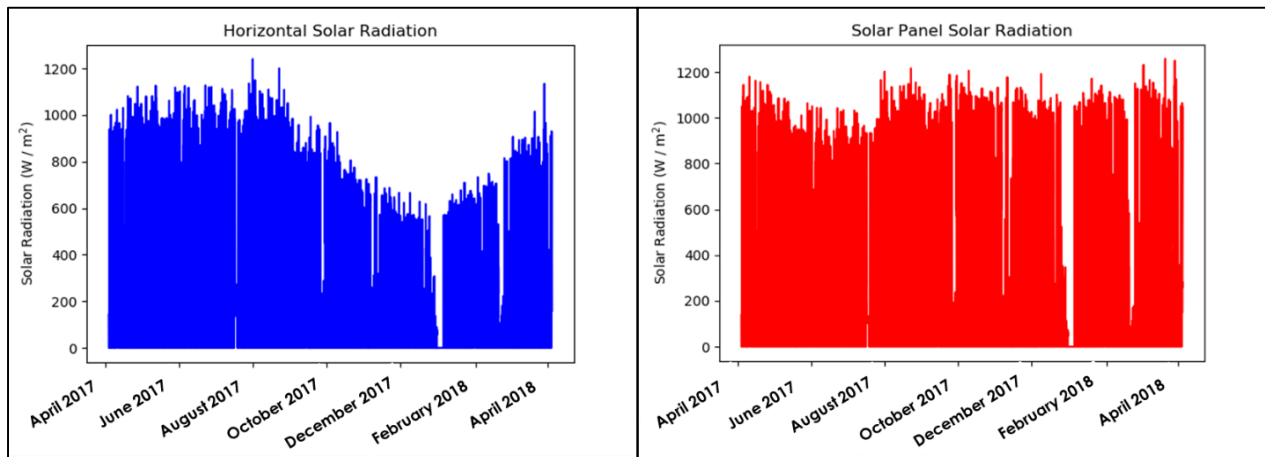
$$\alpha = (90 - \varphi + \delta), \quad (3)$$

where δ is the declination angle, d is the number of the day of the year with January 1st as $d = 1$, φ is the latitude of the site (i.e., 35.236°), and α is the elevation angle. With the elevation angle, horizontal solar radiation (SRAD), and solar panel tilt angle, we can calculate the expected solar radiation at the solar panel (Duffie and Beckman, 1980):

$$\text{Exp. SPSRAD} = \frac{SRAD \times \sin(\alpha + \beta)}{\sin(\alpha)}, \quad (4)$$

where β is the tilt angle of the solar panel (i.e., 47 degrees). These equations describe the direct solar radiation, while the indirect, or diffuse radiation is not affected by the panel orientation. Jacovides et al. (2005) describe methods to estimate the direct and diffuse radiation from the pyranometer data based on a clearness index, which can be verified using our dataset but is beyond the scope of this project.

Figure 2. By tilting the solar panel and the pyranometer 47 degrees and making them face south, the winter's solar radiation is maximized.



In this study, we calculated the relationship between the horizontal solar radiation and the solar radiation at the tilted solar panel. Then, with the output measurements of current and voltage from the solar panel, typical power calculations were made to obtain the wattage in intervals of 5 minutes (DC Watts):

$$Power = I * V, \quad (5)$$

where I is the current (A) and V is the voltage (V). We analyzed how this power output is related to the solar radiation in the tilted surface and with this relationship, we were able to calculate an estimate of the power output based on the solar radiation.

A Photovoltaic (PV) module (i.e., solar panel) consists of individual solar cells electrically connected, but the encapsulation of solar cells into a module may alter the heat flow into and out of the module. This alteration increases the operation temperature of the solar panel and can result in a reduction of its voltage that lowers the output power (PV Education 2018).

Calculations can be made to estimate the solar cell's temperature based on the air temperature obtained from the standard Mesonet's data, according to the following equation:

$$T_{cell} = T_{air} + \frac{(NOCT-20)*S}{80}, \quad (5)$$

where T_{air} is the air temperature from the standard Mesonet's data, $NOCT$ is the Nominal Operation Cell Temperature (i.e., 47 °C), and S is the insolation in mW/cm^2 .

To assess the temperature dependency of our test solar panel, the experimental data from the solar panel's temperature sensor was used. The efficiency of the solar panel was calculated by using the estimate of power output and the actual observed power output when the solar radiation on the panel was more than 200 W/m^2 . We evaluated the relationship between the temperature of the solar panel and the efficiency of the solar panel.

While making all the calculations and analysis, seasonal variations in the elevation of the sun in the sky were considered. All the results were later applied to different cases and different

sizes of arrays to analyze the potential for solar energy production in utility-scale projects.

3. RESEARCH RESULTS

To properly analyze the solar energy potential as determined from our year-long dataset, we focused on gaining robust statistics on the relationship between observations of horizontal and tilted solar radiation, between power generation and observed solar radiation, and between panel temperature and panel efficiency.

3.1. Horizontal solar radiation and solar radiation on a tilted surface

Using over 100,000 observations for solar radiation during our study period, we created the scatter plot shown in Fig. 3. It was immediately obvious that the relationship between horizontal solar radiation and the solar panel's solar radiation (i.e., tilted at 47 degrees) was seasonally dependent.

Because of the tilt of the solar panel's pyranometer, the fall and winter seasons exhibited greater incident solar radiation on the panel compared to the horizontal solar radiation (e.g., see yellow and blue curves). In contrast, during the spring and the summer, the solar radiation observed on a tilted surface was slightly less than that on a horizontal surface (e.g., see red and green curves). As a result, the tilt of a fixed solar panel is critical.

Figure 3. Seasonal relationship between horizontal solar radiation (W/m^2) and solar radiation on a tilted surface (47 degrees).

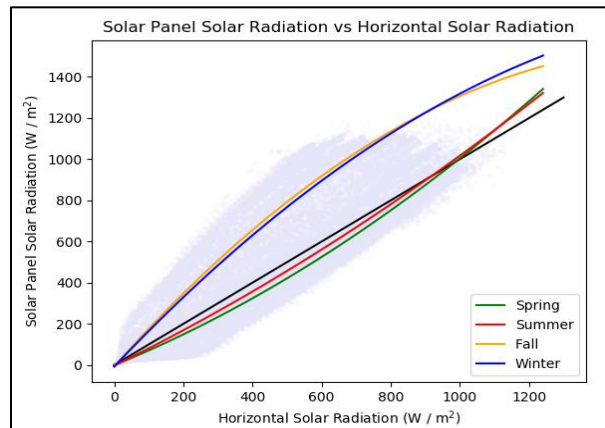
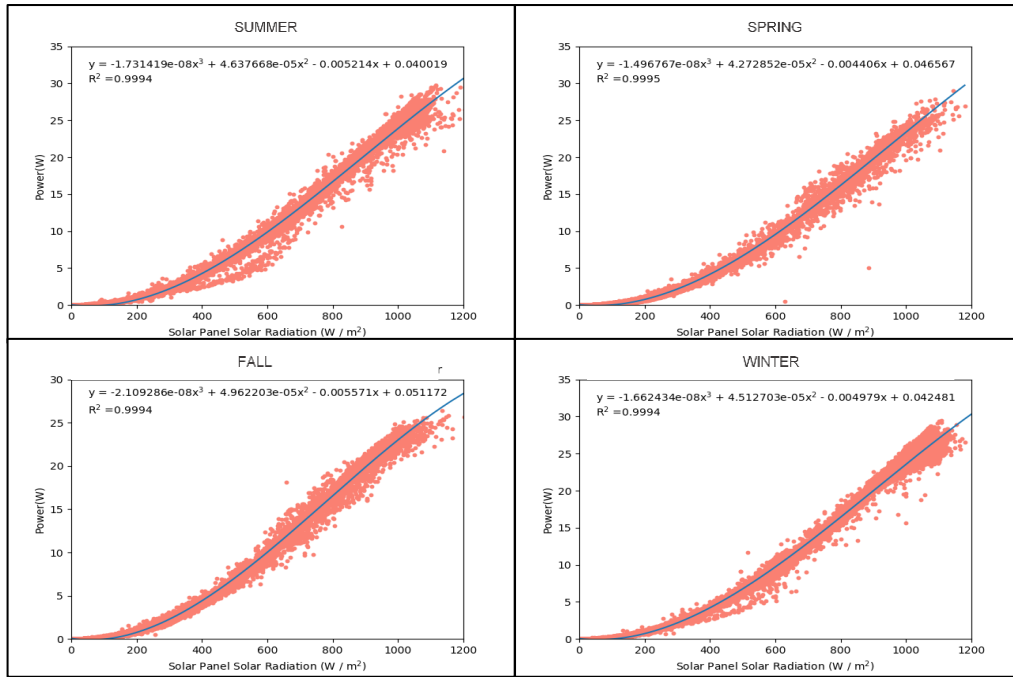


Figure 4. Seasonally relationship between the solar panel's power output (W) and the solar radiation (W/m²) on a tilted surface (47 degrees).



3.2. Power and solar radiation

To determine the relationship between power and observed solar radiation, we generated cubic curves using over 25,000 observations from the different seasons. Figure 4 shows the cubic fit equation and graph for each season. These polynomials can be used to calculate an estimate of power based on the solar radiation at the solar panel for each season. These equations show great promise since R-squared values for the curves show that they are accurate estimates.

3.3. Temperature dependency

To explore the temperature dependency of our solar panel, we calculated the ratio between the observed power and the expected power (i.e., calculated using the polynomial based on the solar radiation). We plotted that ratio as a function of the solar panel's temperature and highlighted the mean values in each 10 °C interval. Our results showed that the panel's power efficiency was stable over the temperature range (Fig. 5).

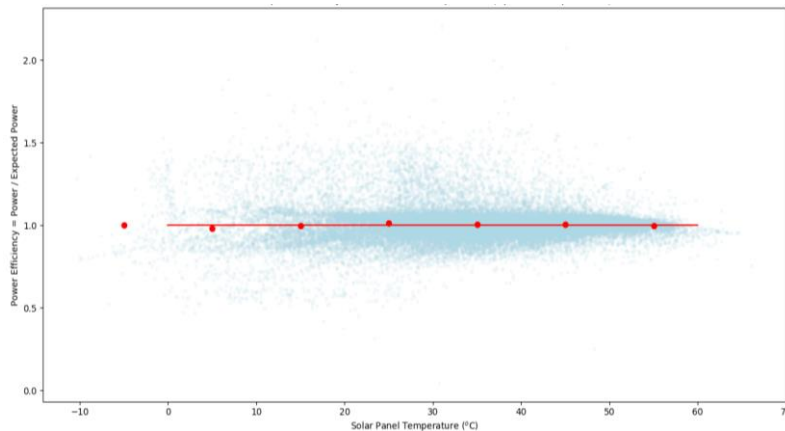


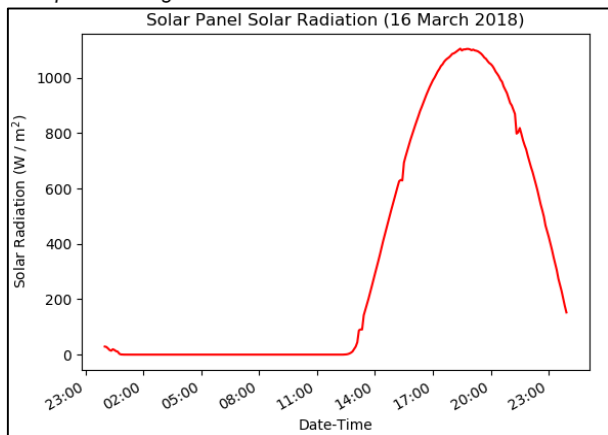
Figure 5. Temperature dependency of the solar panel's efficiency for power output

This finding was somewhat unexpected since manufacturer specifications indicated a temperature dependency (e.g., power production should decrease as temperatures exceeded 47 °C). We hypothesize that the lack of temperature dependence may be due to the age of our test solar panel or to the heat flow between the solar panel and the temperature sensor.

4. HIGHEST SOLAR RADIATION DAY VS. LOWEST SOLAR RADIATION DAY

According to the Mesonet’s archive, the day with the highest solar radiation accumulation was 24 May 2017. However, the Mesonet’s data are based on the horizontal solar radiation, and our interest was focused on the solar radiation at a tilted surface. We found the highest average total solar radiation accumulation at the 47 degrees tilted surface was 29.01 MJ/m², observed on 16 March 2018. In Fig. 6, we show a graph of solar radiation as a function of time for this day. The smooth curve tells us there were few or no clouds during the day, resulting in optimal solar energy potential.

Figure 6. Solar radiation (W/m²) at 47 degrees tilted solar panel during 16 March 2018.

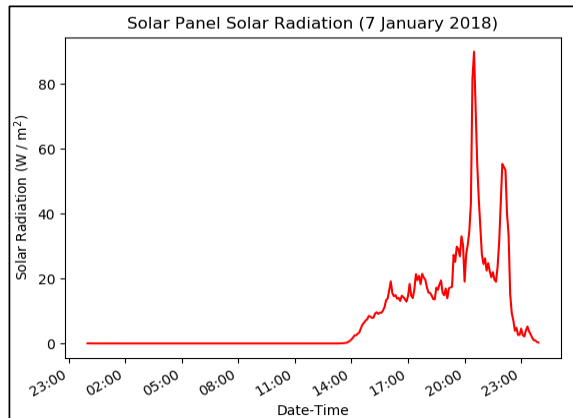


Even though 16 March 2018 was the day with the highest accumulation of solar radiation, it was not the day with the highest accumulation of energy. Yet, it was between the highest 4% for observed energy accumulation for the year, with an accumulation of 0.161 kWh.

In contrast, on 7 January 2018, we observed the lowest average total solar radiation accumulation: 0.668 MJ/m². In its graph of solar radiation as a function of time (Fig. 7), it can be observed how the cloudiness of the day affected the reception of solar radiation at the pyranometer. In fact, this

was also the day with the lowest accumulation of energy with 0.0002 kWh.

Figure 7. Solar radiation (W/m²) at 47 degrees tilted solar panel during 7 January 2018.



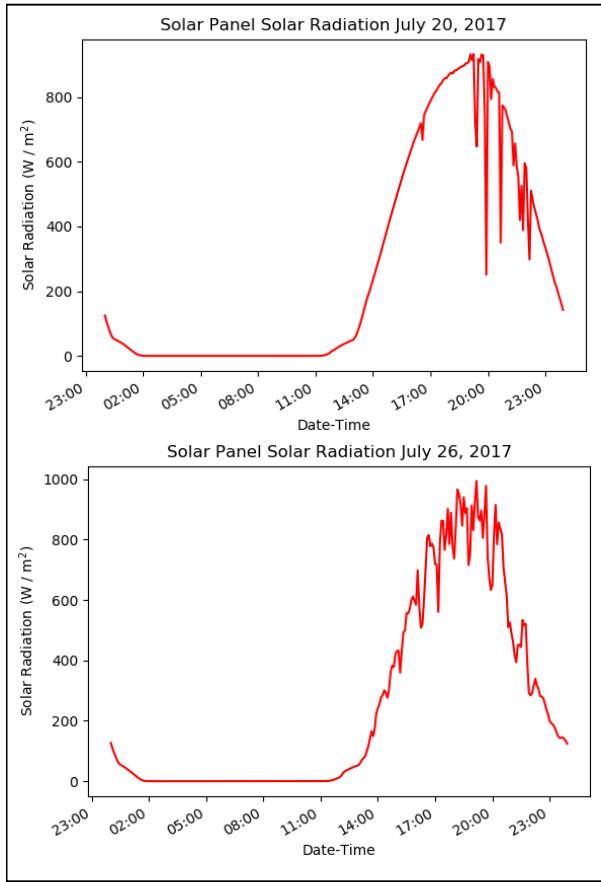
5. CRITICAL DEMAND DAYS

As part of the SmartHours program of Oklahoma Gas and Electric (OG&E), a *critical event* is declared when customer demand for energy is expected to be high, which in Oklahoma generally occurs on hot summer afternoons (OG&E Energy 2018). Customers on the SmartHours program are then charged much higher prices during the hours of 2 pm to 7 pm CDT (19 to 00 UTC) in order to curb peak demand that might otherwise exceed their ability to produce and distribute electricity on the grid. To analyze the potential for solar energy production during peak demand on critical days, we examined the estimated energy production on two of the OG&E-declared critical days during the study period: 20 July 2017 and 26 July 2017 (Fig. 8).

According to the Mesonet’s data archive, the two critical days were in the highest 10% and 20% percentiles (respectively) for observed horizontal solar radiation for the year. Using the solar radiation recorded at the solar panel with the tilt angle, we calculated an average total accumulation of 23.05 MJ/m² for 20 July, and an average total accumulation of 21.07 MJ/m² for 26 July.

Table 1 and Table 2 show the estimated energy generation in a home unit scale and in a utility scale array for both 2017 critical days between 2 pm to 7 pm based on the observed power output in the 30 W solar panel tilted at 47 degrees from the experiment.

Figure 8. Solar Panel Solar Radiation (W/m^2) for each hour (UTC) during critical days: 20 July and 26 July 2017 at the National Weather Center Mesonet site.



	Solar Panel	Home Production	Utility Scale Production
Number of panels	1	200	10,000
Expected Power (DC Watts)	30 W	6,000 W	300,000 W
Observed Average Power	9.8 W	1,960 W	98,000 W
Observed Accumulated Energy	0.049 kWh	9.8 kWh	490.37 kWh

Table 1. Potential energy production with different sizes of arrays for critical day 20 July 2017

	Solar Panel	Home Production	Utility Scale Production
Number of panels	1	200	10,000
Expected Power (DC Watts)	30 Watts	6,000 Watts	300,000 Watts
Observed Average Power	8.12 Watts	1,624 Watts	81,200 Watts
Observed Accumulated Energy	0.0406 kWh	8.12 kWh	405.84 kWh

Table 2. Potential energy production with different sizes of arrays for critical day 26 July 2017

6. SUMMARY AND FUTURE WORK

Using observed data from the Oklahoma Mesonet and data from a field experiment, we analyzed the solar insolation and solar energy production at an Oklahoma Mesonet site. A seasonal variation was observed throughout the year when analyzing the relationship between the horizontal solar and the solar radiation at a tilted solar panel. Thus, the optimal tilt angle of a solar panel will depend on the latitude and the time of the year in which the solar energy is needed. It was demonstrated that the power output of a solar panel can be defined by a cubic equation based on the solar radiation received at the solar panel.

We also found no temperature dependency on the efficiency of our test solar panel. Two of the possible explanations for this behavior are the solar panel's age and the lack of heat flow between the panel and the temperature sensor.

Future work will include estimating the direct and diffuse radiation from the pyranometer data based on a clearness index and verifying it with our data. It is also of interest to use tracking solar systems to assess how solar panel orientation might change the power production curve. Using the power estimations based on solar radiation, we want to analyze the potential for solar energy production across Oklahoma, and then apply our findings in other locations around the world.

7. ACKNOWLEDGMENTS

The authors would like to thank Dr. Daphne LaDue for her support in the National Weather Center Research for Undergraduates Program, and the taxpayers of Oklahoma for their continued support of the Oklahoma Mesonet. Also, the corresponding author would like to personally thank Michael Klatt, Nicholas Szapiro and Brad Illston for their assistance in the coding used in the analysis, and, Melanie Schroers and

Jacqueline Waters for their guidance and advice during this experience. Additionally, we thank the Oklahoma Climatological Survey for their hosting and the entire Oklahoma Mesonet Staff and Quality Assurance team for providing and maintaining the data.

This work was prepared by the authors with funding provided by the National Science Foundation Grant No. AGS-1560419.

8. REFERENCES

- American Wind Energy Association, 2017: U. S. Wind Energy State Facts. Accessed online: 10 July 2018. <http://www.awea.org/resources/statefactsheets.aspx?itemnumber=890&navItemNumber=5067>.
- Brewster, K. A., and S. K. Degelia, 2016: Availability and Variability of Potential PV Solar and Wind Power Production in Oklahoma., *Preprints of 7th Conference on Weather Climate and the New Energy Economy*, Amer. Meteor. Soc., Paper 3.3.
- Duffie, J. A., and W. A. Beckman, 1980: *Solar engineering of thermal processes*. Wiley, 762 pp.
- Energy Information Administration, 2018: Renewable Energy Production and Consumption by source. Accessed online: 29 June 2018. <https://www.eia.gov/totalenergy/data/browser/?tbl=T10.01#/?f=M&start=200001>.
- Jacovides, C. P., F. S. Tymvios, V. D. Assimakopoulos, N. A. Kaltsounides, 2006: Comparative study of various correlations in estimating hourly diffuse fraction of global solar radiation. *Renewable Energy*, **31**, 2492-2504.
- Li, W., S. Stadler, and R. Ramakumar, 2011: Modeling and Assessment of Wind and Insolation Resources with a Focus on their Complementary Nature: A Case Study of Oklahoma. *Annals of the Association of American Geographers*, **101**, 4, 717-729.
- McPherson, R. A., C. A. Fiebrich, K. C. Crawford, R. L. Elliott, J. R. Kilby, D. L. Grimsley, J. E. Martinez, J. B. Basara, B. G. Illston, D. A. Morris, K. A. Kloesel, S. J. Stadler, A. D. Melvin, A.J. Sutherland, and H. Shrivastava, 2007: Statewide Monitoring of the Mesoscale Environment: A Technical Update on the Oklahoma Mesonet. *J. Atmos. Oceanic Technol.*, **24**, 301-321
- OGE Energy, 2018: SmartHours. Accessed online: 15 July 2018. https://www.oge.com/wps/portal/SignIn!/ut/p/a1/04_Sj9CPykssy0xPLMnMz0vMAfGjzOltjAycDTxNjLzcvY1cDRy9XVwCTQNcDD2NzYAKIoEKDHAARwNC-sP1o8BK8JhQkBthkO6oqAgArHFgDg!!/dl5/d5/L2dBISEvZ0FBIS9nQSEh/.
- PV Education, 2018: Solar Radiation on a Tilted Surface. Accessed online: 15 June 2018. <https://www.pveducation.org/pvcdrom/properties-of-sunlight/solar-radiation-on-a-tilted-surface>.
- Reichling, J.P., and F. A. Kulacki, 2008: Utility scale hybrid wind-solar thermal electrical generation: A case study for Minnesota. *Energy*, **33**: 4, 626-638, DOI: <https://doi.org/10.1016/j.energy.2007.11.001>
- U.S. Department of Energy, 2018: Renewable Energy: Solar. Accessed online: 29 June 2018. <https://www.energy.gov/science-innovation/energy-sources/renewable-energy/solar>.
- Van der Veer Martens, B., B. G. Illston, and C. A. Fiebrich, 2017: The Oklahoma Mesonet: A Pilot Study of Environmental Sensor Data Citations. *Data Science Journal*, **16**: 47, 1–15, DOI: <https://doi.org/10.5334/dsj-2017-047>.